PNAS RESEARCH ARTICLE | DEVELOPMENTAL BIOLOGY

Chinmo is the larval member of the molecular trinity that directs *Drosophila* metamorphosis

James W. Truman[a] and Lynn M. Riddiford[a,1]

Contributed by Lynn M. Riddiford; received January 19, 2022; accepted March 2, 2022; reviewed by David Martin, Frederik Nijhout, and Stuart Reynolds

The molecular control of insect metamorphosis from larva to pupa to adult has long been a mystery. The Broad and E93 transcription factors, which can modify chromatin domains, are known to direct the production of the pupa and the adult, respectively. We now show that *chinmo*, a gene related to *broad*, is essential for the repression of these metamorphic genes. *Chinmo* is strongly expressed during the formation and growth of the larva and its removal results in the precocious expression of *broad* and *E93* in the first stage larva, causing a shift from larval to premetamorphic functions. This trinity of Chinmo, Broad, and E93 regulatory factors is mutually inhibitory. The interaction of this network with regulatory hormones likely ensures the orderly progression through insect metamorphosis.

Broad | E93 | Krüppel-homolog 1 | juvenile hormone

Significance

The genome of insects with complete metamorphosis contains the instructions for making three distinct body forms, that of the larva, of the pupa, and of the adult. However, the molecular mechanisms by which each gene set is called forth and stably expressed are poorly understood. A half century ago, it was proposed that there was a set of three master genes that inhibited each other's expression and enabled the expression of genes for each respective stage. We show that the transcription factor *chinmo* is essential for maintaining the larval stage in *Drosophila*, and with two other regulatory genes, *broad* and *E93*, makes up the trinity of mutually repressive master genes that underlie insect metamorphosis.

Insects evolved from Crustacean stock about 450 Mya and diversified to become a major group of animals that profoundly shaped the subsequent evolution of plant and animal life in the terrestrial biosphere (1). A major feature of insect success was through their development of metamorphosis (1–3). Initially, insects had a direct developing (ametabolous) life history, like today's silverfish (Zygentoma), in which the hatchling is a miniature version of the adult, with little change in body form during growth except for the eventual appearance of genitalia needed for adult reproduction. The evolution of wings and powered flight resulted in further modifications of postembryonic development. In this hemimetabolous pattern, development is still direct because the hatchling, which is typically called a nymph, acquires the basic body form of the adult, but it lacks wings as well as genitalia. These structures gradually appear as wing and genital pads as the nymph grows and are transformed into the adult structures at the final molt. The subsequent evolution of a holometabolous life history, with discrete larval, pupal, and adult stages, then involved a profound shift in embryonic development. Embryogenesis no longer produced a miniature version of the adult that laid the egg, but it was somehow redirected to generate a strikingly different body plan, like that of the caterpillar versus its parent butterfly. The larva goes through successive growth stages using this modified form, and the adult body plan is finally established at metamorphosis after larval growth is complete.

There are longstanding, conflicting views about how the holometabolous pattern evolved from an ancestral hemimetabolous pattern. One view is that there was a gradual transition in which selection pressures on the nymph promoted a divergence of form away from that of the adult, and this disparity eventually became so great that it required the interposition of a transitional stage in-between which is now known as the pupa (1, 4, 5). In this view, larvae and nymphs are considered equivalent, differing only quantitatively across a large spectrum. Support for the equivalence of larvae and nymphs is twofold: (1) the presence of juvenile hormone (JH) in the immature stages enforces molting to another immature stage and the decline of JH during the final nymphal or larval instar allows metamorphosis (5); and (2) the transcription factor *Krüppel-homolog 1* (*Kr-h1*), which mediates JH action (6), serves to maintain both larval and nymphal stages and must disappear from both for metamorphosis to occur (5–7). The alternate view, formulated over a century ago (8), is that the holometabolous shift involved a fundamental alteration in embryogenesis that suppressed the production of the species-typical, imaginal form and allowed the development of an altered body form (9). This shift allowed the uncoupling of the development of the immature and mature stages so that selection could now act on each independently, thereby providing the opportunity for a profound divergence in the forms of the two stages (10). In this view, the larva was the evolutionary innovation; it became the stage devoted to growth, while the nymphal stages were eventually reduced to a single, nonfeeding, transition stage (i.e., the pupa) in which the adult body plan forms. Interestingly, two hemimetabolous orders (the thrips, Thysanoptera, and some scale insects and white

Author affiliations: [a]Friday Harbor Laboratories, University of Washington, Friday Harbor, WA 98250

Author contributions: J.W.T. and L.M.R. designed research; J.W.T. and L.M.R. performed research; J.W.T. and L.M.R. analyzed data; and J.W.T. and L.M.R. wrote the paper.

Reviewers: D.M., Universitat Pompeu Fabra; F.N., Duke University; and S.R., University of Bath Department of Biology and Biochemistry.

The authors declare no competing interest.

See online for related content such as Commentaries.

[1]To whom correspondence may be addressed. Email: lmr@uw.edu.

This article contains supporting information online at http://www.pnas.org/lookup/suppl/doi:10.1073/pnas.2201071119/-/DCSupplemental.

Published April 4, 2022.

flies within the Hemiptera) have also evolved a holometabolous-like lifestyle (termed neometaboly) (1, 4, 11), but in these cases, the transition from larva to adult requires two or three nonfeeding, pupa-like stages, rather than just one.

In a theoretical paper, 50 y ago, Williams and Kafatos (12) proposed that the larval, pupal, and adult stages were each controlled by their own master regulatory gene that controlled access to stage-specific gene sets. These three master genes reciprocally inhibited each one another and were responsive to the suite of hormones that regulated metamorphosis. We now know that many "stage-specific" genes such as the cuticle genes may be expressed in one, two, or all three of these stages depending on the nature of the cuticle being produced (13), but master controlling genes have not been ruled out. Genetic and molecular approaches have recently identified some members of this trinity of master genes (Fig. 1*A*). The first master gene was the *broad* gene, a Broad-Tramtrack-Bric-á-brac (BTB) domain-C_2H_2-zinc-finger transcription factor that is both necessary and sufficient for production of the pupal stage of *Drosophila melanogaster* (14, 15). Indeed, the expression of *broad* is a universal feature of the holometabolous pupa (1, 9) and is also found in the pupa-like stages of neometabolous forms (11). Interestingly, *broad* is also expressed in hemimetabolous nymphs, first appearing in early embryogenesis and continuing until the start of the last nymphal stage in preparation for metamorphosis (1, 9, 16–18). While this expression apparently links the hemimetabolous nymph with the holometabolous pupa, there are species differences as to whether its RNA interference (RNAi)-mediated knockdown can precociously cause entry to the adult stage (1, 9, 16). Hence, it is not clear if *broad* is a master gene for both. The second master gene was *ecdysone-inducible protein 93F* (*eip93F*, commonly known as *E93*) which encodes a Pipsqueak-family transcription factor. It is essential for the formation of the adult stage of *Drosophila* and the beetle, *Tribolium castaneum*, as well as of hemimetabolous insects (1, 19–21).

The identity of a larval member of this trinity has been more problematical. Holometabolous larvae differ from nymphs in that they do not express *broad*, except for a subset of neurons in the central nervous system (CNS) (9, 22). Larvae do express *Kr-h1* and its loss in later larval instars causes premature metamorphosis as does the removal of JH (1, 6, 7, 9). However, do such results mean that Kr-h1 is the larval master gene or is Kr-h1 the link that allows JH to maintain expression of such a gene? Importantly, the removal of Kr-h1 in *D. melanogaster* does not prevent the formation of the larva or the progression through the larval instars (23). Also, the suppression of JH production or action in embryos of the silkworm *Bombyx mori* results in production of normal larvae and these larvae can progress through the next two larval instars despite the absence of JH and *Kr-h1* expression (24). Lastly, after metamorphosis begins in the Holometabola, JH and Kr-h1 return to regulate aspects of pupa formation (9, 21). Indeed, the expression of Kr-h1 is tightly associated with JH and not with the particular stage on which JH acts.

If not *Kr-h1*, then what is the gene that specifies the larval stage? A recent report by Syed et al. (25) showed that early, intermediate and late neuronal phenotypes generated by *Drosophila* mushroom body neuroblasts were associated with the sequential expression of three transcription factors, *chinmo* (chronologically inappropriate morphogenesis), *broad*, and *E93*, respectively. Because the last two transcription factors are master genes for the pupa and adult stages, we wondered if Chinmo might have a similar role for the larval stage. *Chinmo*

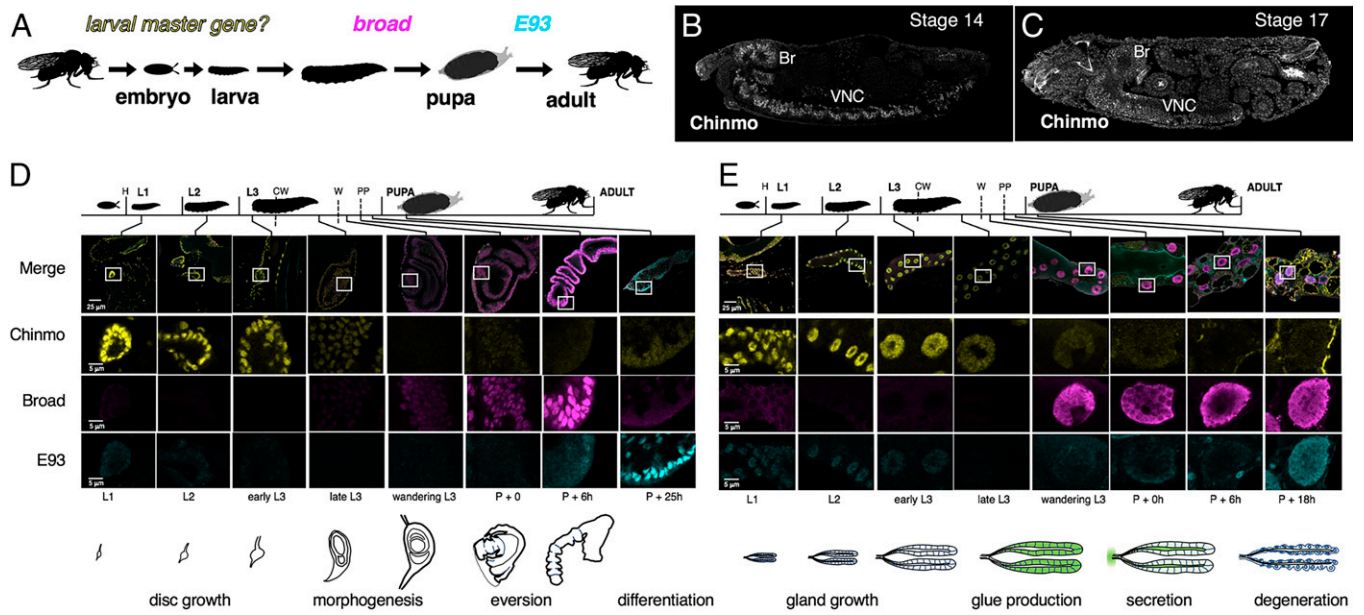

Fig. 1. The relationship of the master regulatory genes to the life stages of *Drosophila*. (*A*) The transcription factor and chromatin-modifying genes *broad* and *eip93F* (*E93*) oversee the formation of the pupal and adult stages, respectively, but the existence of a corresponding gene for the larval stage is unclear. (*B* and *C*) Lateral views of a Stage 14 (*B*, ~11 h after fertilization) and a mid-Stage 17 embryo (*C*, a few hours before hatching). Chinmo-IR first appears in the brain and ventral nerve cord (*B*) but is later found in all tissues (*C*). (*D* and *E*) Confocal optical sections of triple-stained leg imaginal discs (*D*) or the salivary glands (*E*) at various times during larval growth, pupation, and the early phases of adult differentiation. Upper panel: a low-power merged image indicating the boxed area which shows the separate channels for Chinmo (yellow), Broad (magenta), and E93 (cyan) immunoreactivity. Chinmo levels decline in the third larval stage (L3) at the critical weight checkpoint (CW). Broad becomes especially prominent late in wandering (W, wandering L3) and at pupariation (PP). E93 levels rise after the formation of the pupa. The salivary glands are well into degeneration by 18 h after pupariation (P+18h). L#, # larval stage; early and late L3, feeding larvae before and after the critical weight checkpoint; P+#h, number of hours after pupariation. Diagrams show the appearance of the leg imaginal disc (left) and salivary glands (right) through larval life and the initiation of adult differentiation. The green in the salivary gland indicates the production of glue protein late in larval life.

was initially identified by its action in controlling temporal identity of progeny from postembryonic neuroblasts (26). Also, the critical weight checkpoint that ushers in the start of metamorphosis in the last larval stage causes a switch-over from *chinmo* to *broad* expression in neuronal lineages (22, 27) and also in imaginal discs (28), where the two genes have mutually antagonistic interactions. We set out to see if *chinmo* might be the larval member of the holometabolous trinity through further analysis of its expression and genetic deletion experiments.

Results

Based on whole-body mRNA and protein measurements in ModEncode (29), *chinmo*, *broad*, and *E93* expression are associated with the three successive phases of the *Drosophila* life history. Chinmo immunoreactivity first appears in the CNS as the embryo is undergoing germband retraction (Stage 14; ∼11 h after fertilization) and is ubiquitously expressed by hatching (Fig. 1 *B* and *C* and *SI Appendix*, Fig. S1). Except for neurons, larval cells of *Drosophila* are polyploid and grow by cell enlargement during the three larval stages (L1 to L3), but most then degenerate early in metamorphosis. Larvae also possess clusters of diploid imaginal cells that form the imaginal discs and primordia. These do not make larval structures but proliferate during larval growth and eventually replace the larval cells to make the adult body. In both larval cells and imaginal disc cells (Fig. 1 *D* and *E*), Chinmo levels are high from hatching through the early part of L3, until the larva passes the critical weight checkpoint that is the entry into metamorphosis (∼8–10 h into L3 stage) (30). At this time, Chinmo levels begin to decline in both imaginal discs and larval cells (Fig. 1 *D* and *E*) (28) and *broad* isoforms appear. This change-over has been studied in the premetamorphic wing imaginal disc, where Chinmo and Broad reciprocally inhibit each other, such that the experimental suppression of one causes the elevated expression of the other (28). Broad is prominent in both larval and imaginal cells during the formation of the pupal stage and then E93 appears in both cell types as adult differentiation is under way (Fig. 1 *D* and *E*). The larval cells then degenerate while Broad protein is still present (Fig. 1*E*), but imaginal disc cells completely replace Broad with E93 as the adult structures differentiate (Fig. 1*D*).

Chinmo first appears around midembryogenesis and *Chinmo* mutants are embryonic lethal (26). We examined the phenotype of the *chinmo*^{1} mutant, using the balanced line used for Chinmo MARCM (mosaic analysis with a repressible cell marker) studies (*w**; *chinmo*^{1} *P* {*ry*$^{+t7.2}$ = *neoFRT*} *40A*/*CyO*, *y*$^{+}$) (hereafter called *chinmo*^{1}/*CyO*) (26) (see *SI Appendix*, Table S1 for *Drosophila* lines and abbreviations used). When this line was crossed to itself, approximately half of the larvae hatched (Fig. 2*A*), 90% of which showed strong Chinmo-immunoreactivity (IR) (Fig. 2 *B* and *C*; *chinmo*^{1}/*CyO*). Approximately one quarter of the eggs showed no obvious embryo (presumably *CyO*/*CyO*), and the remaining quarter blocked in late embryogenesis. One set of late-arresting embryos (Class I) appeared to be fully developed with gas filling their tracheal systems, while a second set (Class II) showed a gut configuration similar to a Stage 15 embryo but with sclerotized mouth hooks and obvious denticle belts. Immunostaining for Chinmo showed that many Class I embryos had the depressed levels of Chinmo expression expected for the *chinmo*^{1}/*chinmo*^{1} homozygote (Fig. 2*B*). Crossing *chinmo*^{1} to different deletion lines that removed the entire locus yielded only the Class I phenotype (Fig. 2*A*). Many of the Class I embryos expelled Malpighian tubule contents into the space between the embryo and the vitelline membrane, and these embryos all showed depressed levels of Chinmo (Fig. 2*B*). Most of these embryos had normal proportions but others were shortened along their anterior-posterior axis.

The *chinmo*^{1} mutant was thought to be a protein null based on the lack of Chinmo-IR in homozygous *chinmo*^{1} neuroblast clones (26), but our data suggest that it is a hypomorph. We think that the clones in the previous study lacked Chinmo expression because the mutant neuroblasts had shifted into making their late-born progeny, which are normally Chinmo-negative. Crossing *chinmo*^{1}/*CyO* flies to either deletion stock also produced late arrested embryos with very low levels of Chinmo-IR (Fig. 2*C*, *chinmo*^{1}/*Df*); while embryos with the overlapping deletions, which completely removed the *chinmo* locus, showed no Chinmo-IR (Fig. 2*C*, *Df*/*Df*). A few *chinmo*^{1} homozygotes apparently hatch because we found occasional hatchlings from these crosses with very low Chinmo expression (Fig. 2*B*). However, we found no mid- or late-stage L1 larvae that showed low Chinmo expression, suggesting that these *chinmo*^{1} homozygotes do not grow.

The phenotypes of the *chinmo*^{1} homozygotes and the double deletion embryos show that zygotically produced Chinmo is not needed to form the larva, but because such animals die, they cannot tell us if Chinmo is needed to maintain the larval state. Consequently, we turned to a mosaic approach in which we removed Chinmo from only some larval cells and then tracked their development in the growing animal. We used an *engrailed-GAL4* driver to express a nuclear localized red fluorescent protein (nRFP) marker and *chinmo RNAi* constructs (*SI Appendix*, Table S1) in the posterior compartments of larval body segments and imaginal discs. Two independent lines, *UAS-TRiP HMC05346* and *UAS-TRiP HMS00036*, resulted in marked depletion of Chinmo-IR in the Engrailed-positive compartments. The former gave the stronger knockdown of Chinmo-IR and was the principal line used for these studies. As seen in Fig. 2 *D* and *E*, cells that lacked Chinmo in the first larval instar showed the precocious expression of either Broad or E93, the genes that normally are expressed at the onset of metamorphosis to pupal (14, 15) or adult (20) stage, respectively (Fig. 1 *D* and *E*). However, the imaginal disc and larval cells differed in which trinity gene they expressed. Larval cells, characterized by epidermal and salivary gland cells, showed premature expression of E93 but not Broad, while the imaginal disc cells showed premature expression of Broad but not E93. We do not yet know the reasons why mutant larval cells precociously express E93 whereas the imaginal cells express Broad, but they may arise from differences in how these later trinity members interact with each other in the respective tissues. Larval and imaginal cells also differed in the timing of their response to the loss of Chinmo. Larval epidermal cells that lacked Chinmo showed precocious E93 expression by about midembryogenesis (late stage 15, shortly after dorsal closure and head involution) (Fig. 2*F*), shortly after the time when Chinmo first appears. In the case of Broad, by contrast, precocious expression in imaginal disc cells did not appear until the mid to late first instar (e.g., Fig. 2*D*). These imaginal disc cells may be basically dormant until stimulated to proliferate late in the first instar (31). This break of dormancy may be necessary for Broad expression to begin. The second *chinmo-RNAi* construct also caused premature expression of Broad in imaginal discs and E93 in larval cells (*SI Appendix*, Fig. S2).

The loss of Chinmo had profound developmental effects on both larval and imaginal disc cells. The *en-GAL4* > *UAS-chinmo-RNAi* (*UAS-TRiP HMC05346*) larvae grew during the L1 stage and eventually achieved a size larger than a young L2,

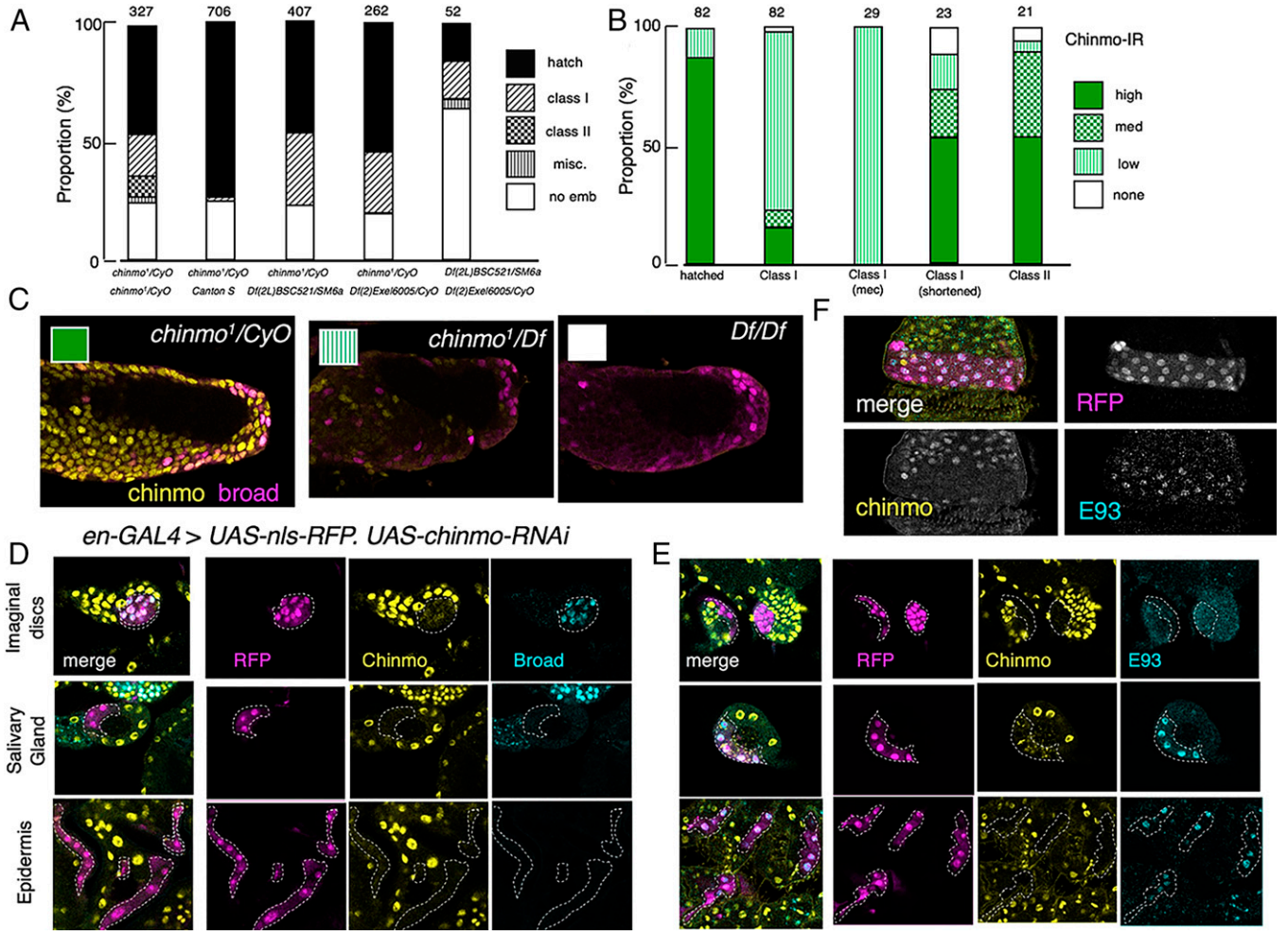

Fig. 2. Effects of the loss of *chinmo* function. (*A–C*) Phenotypes of the progeny of various crosses of *chinmo*^{1}*/CyO* flies to themselves, to wild type (*Canton S*), to various deletions of the *chinmo* gene, or of the overlapping deletions to each other. (*A*) The percentage of eggs that hatched, showed no obvious embryo or had blocked late-stage embryos. The latter typically had either appeared to finish development but were not hatched (Class I) or showed an earlier block having some tissues at about stage 15 but some more advanced features such as sclerotized mouth hooks (Class II). Substantial percentages of Class I, but not Class II, blocked embryos were found in the other four crosses that produced progeny lacking a wild-type *chinmo* gene. (*B*) Levels of Chinmo-IR in the different phenotypic classes. Class I embryos showed low, but detectable levels of Chinmo-IR. Within the Class I set, some embryos released meconium into the subvitelline space (mec) while others showed a pronounced anterior-posterior compression (shortened). These two groups were overlapping. Low Chinmo expression was consistently found in the mec subgroup. (*C*) Confocal images showing examples of high (*chinmo*^{1}*/+*), low (*chinmo*^{1}*/Df(2L)Exel6005*), and no (*Df(2L)BSC521/Df()Exel6005*) Chinmo expression in the embryonic CNS. Scattered Broad expression is seen in all samples. (*D* and *E*) Confocal images of immunostained first instar larvae showing the effects of removing Chinmo by expressing a *chinmo-RNAi* construct under control of an *engrailed-GAL4* driver. Cells expressing the *chinmo-RNAi* are marked by nuclear red fluorescent protein (RFP) expression. L1 imaginal disc cells lacking Chinmo show precocious expression of Broad but not E93, while salivary gland or epidermal cells lacking Chinmo show precocious expression of E93 but not Broad. (*F*) Early expression of E93 is already evident in the Chinmo-negative epidermis of midstage embryos.

but they did not molt to the second instar (Fig. 3*A*). Some of these larvae then assumed a "tiger-striped" appearance, with two thin rings of tanned cuticle within each segmental *engrailed* domain (Fig. 3*B*). These rings correspond to tanned cuticular ridges that normally appear in the last larval cuticle as it transforms into the puparium at the start of metamorphosis (Fig. 3*C*). Optical cross sections through such larvae (Fig. 3*D*, diagrammed in Fig. 3*E*) show that the epidermal cells between *engrailed* domains make a new, L2 cuticle, while the Chinmo-negative cells within each *engrailed* domain did not (and instead started puparial tanning). Consequently, at the end of the first larval stage, the epidermal cells of these mosaic larvae respond to the molting surge of ecdysteroids in different ways depending on whether or not they express *chinmo*: the Chinmo-positive cells make a new larval cuticle (Fig. 3 *D* and *E*) while the Chinmo-negative cells are directed toward metamorphosis and puparial tanning (Fig. 3 *B* and *E*).

Analysis of the knockdown of *chinmo* in the salivary gland shows that Chinmo is also involved in the normal trajectory of cell growth in this tissue. At hatching, nuclear size is the same in wild-type versus Chinmo-negative regions of the salivary gland. Later in the L1 stage, the wild-type cells have grown markedly but the Chinmo-negative cells remain small (Fig. 3*F*).

Chinmo is also involved in the early growth of the imaginal discs. For example, the wing imaginal disc is an invaginated sac of epidermis that shows little distinction between the anterior and posterior compartments at hatching. The wing discs of *en-GAL4 > UAS-nRFP, UAS-chinmo-RNAi* larvae form normally and look like those of wild-type at hatching. Proliferation begins in the wing disc in the late first instar (31), and those from *en-GAL4 > UAS-nRFP* larvae expand as a relatively uniform epithelium (Fig. 3*G*), while those from *en-GAL4 > UAS-nRFP, UAS-chinmo-RNAi* larvae show cells within the RFP domain that are abnormally thickened and disorganized. In

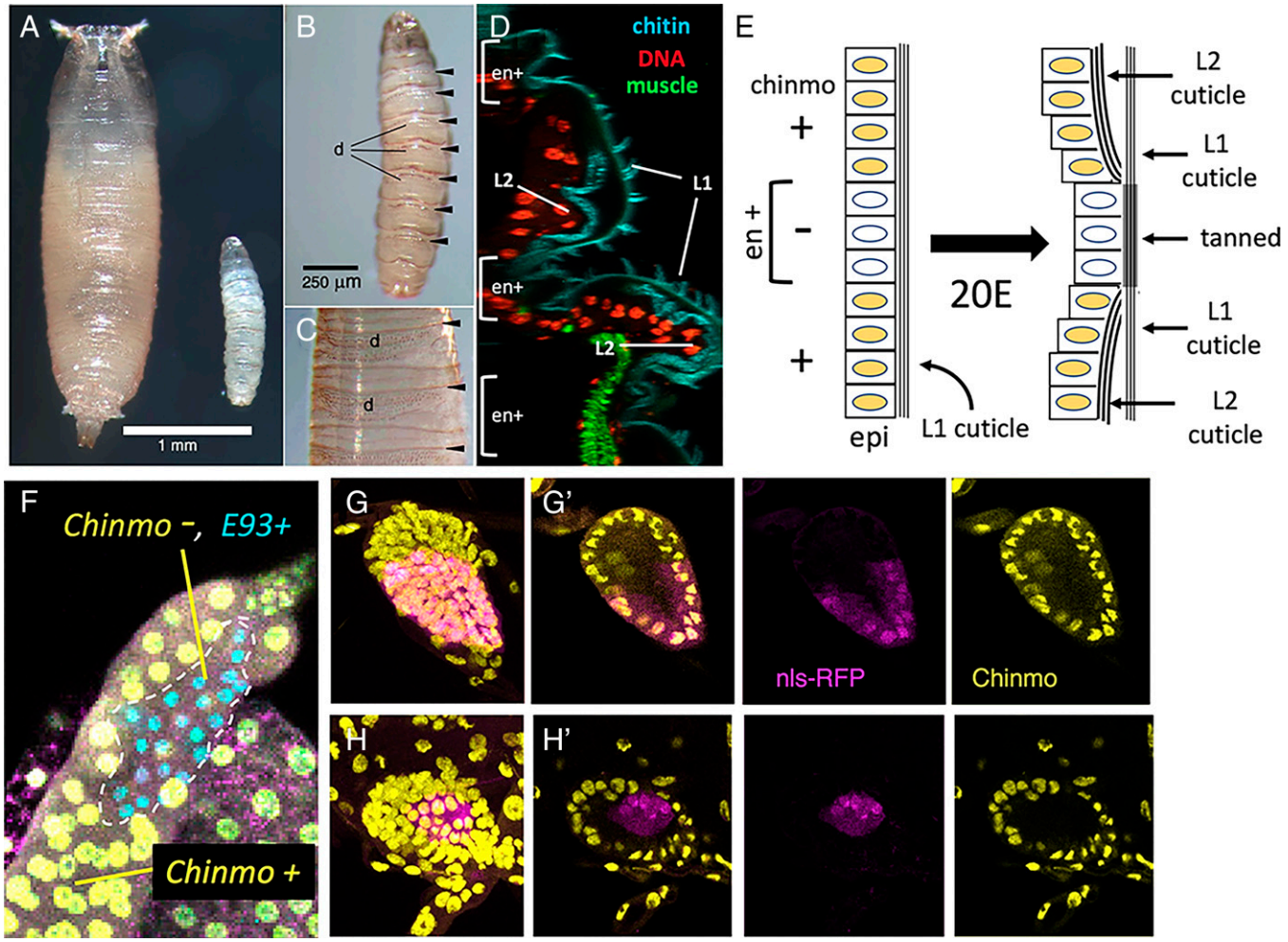

Fig. 3. The growth and development of L1 larvae that carry *engrailed-GAL4*, *UAS-nls-RFP*, and *UAS-chinmo-RNAi* transgenes. (*A*) photomicrograph of the ventral view of a wild-type puparium and a partial, precocious puparium formed by an *en-GAL4* > *chinmo-RNAi* L1 larva. (*B*) High magnification image of the L1 partial puparium from (*A*), showing bands of tanned cuticle in the posterior domain of each segment. Comparison with a normal puparium case (*C*) show that the bands correspond to the ridges found in the posterior compartment of each segment of the puparium; arrowheads: the tanned ridge that marks the posterior border of the engrailed domain and the denticle bands (d) of the next segment. (*D*) A confocal image through the body wall of a L1 partial puparium. Chitin staining shows the continuous outer L1 cuticle whereas the L2 cuticle is laid down in bands in the *engrailed*-negative anterior region of each segment. (*E*) Summary of the molting response of *en-GAL4* > *chinmo-RNAi* L1 larvae; in each segment the anterior compartment cells, which possess Chinmo, make a L2 cuticle while the posterior compartment cells, which lack Chinmo, show the metamorphic response of puparial tanning. (*F*) A confocal section through the L1 salivary gland. The patch lacking Chinmo has nuclei that express E93 but have not grown like their wild-type neighbors. (*G* and *H*) Comparison of late L1 wing discs from *en-GAL4* larvae expressing either *nRFP* (*G*) or *nRFP* and *chinmo-RNAi* (*H*); *G* and *H* are projections through the entire stack while *G*′ and *H*′ are single optical sections through the middle of the disc. The Chinmo-negative cells have been excluded from the epithelium and pushed into the disc lumen.

extreme cases, these latter cells ball-up and are extruded into the disc lumen (Fig. 3*H*). Considering that these cells are expressing Broad, we suspect that they prematurely shift into a premetamorphic mode, although we have not yet found an independent molecular marker to support this conclusion.

Discussion

The life history of holometabolous insects, with their complete metamorphosis, involves a progression through three distinct body forms comprising the larva, the pupa, and the adult, respectively. Single genes, *broad* and *E93*, oversee the formation of the pupal and adult stages, respectively (9, 19). Although these genes are transcription factors, they also are involved in altering the chromatin landscape, opening up regions of DNA relevant to their respective life-stage and closing down regions relevant to the other two (32, 33). This function has been elegantly shown for the actions of E93 in opening up the chromatin landscape needed for the formation of the adult and for closing the chromatin around the *broad* gene (32, 34). Until now, a larval specifier—and hence the first member of the hypothesized larval-pupal-adult specifying trinity of master genes (12)—has remained elusive. Our data suggest that *chinmo* is the first member of the trinity, overseeing the maintenance of the larval stage in holometabolous insects. As a member of the BTB gene family that includes *broad*, Chinmo, like Broad, may mediate maintenance of the larval state through chromatin modification as well as by direct control of gene expression.

Timing of *chinmo* expression is consistent with that expected for a larval control gene (Fig. 4*A*). It appears around embryonic stage 14, during germband retraction and dorsal closure. This time of appearance is significant because the extended germband stage, when body segmentation is complete and the primordia for appendages and the various organ systems have been established, is similar in both hemi- and holometabolous insects (35). In direct developers, this stage is followed by the production of the imaginal body plan, while in insects with a larval stage development is redirected to making the larval

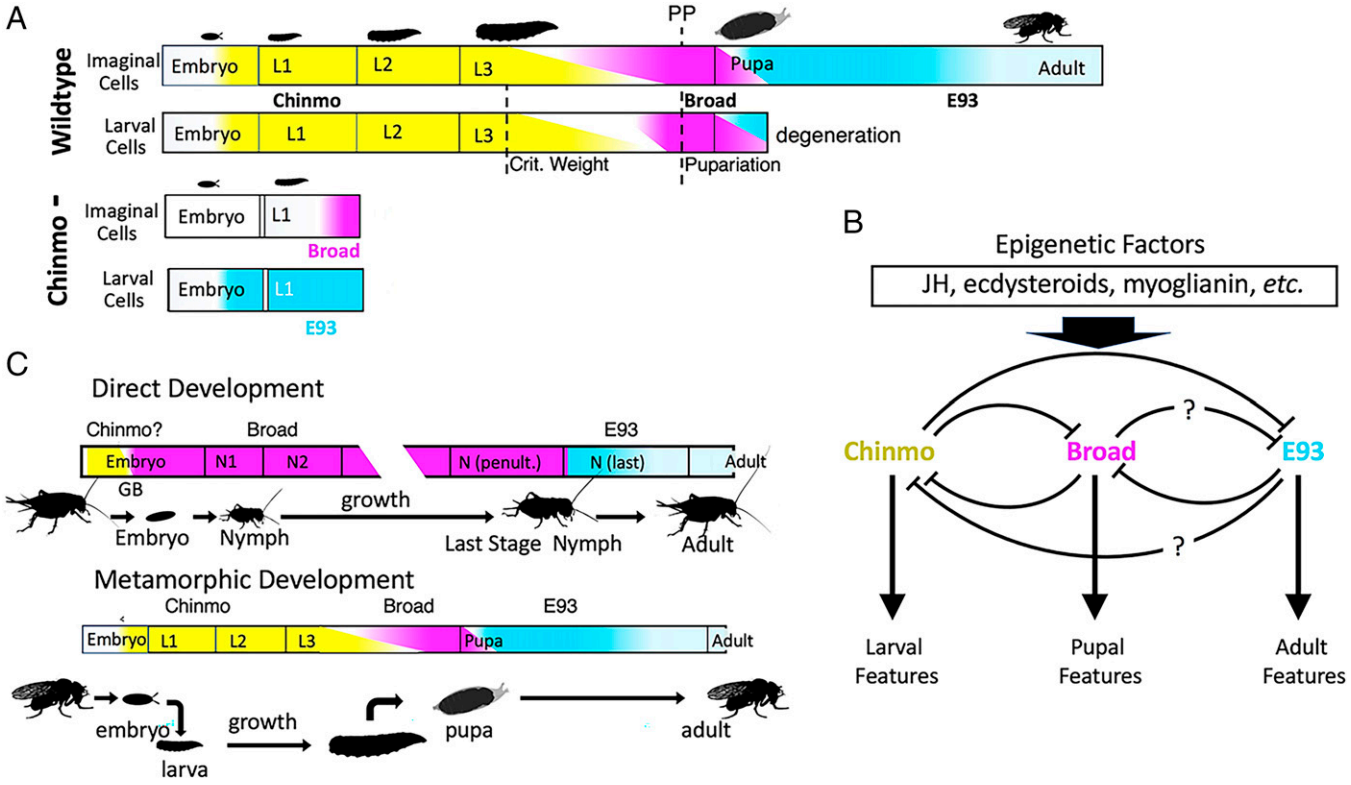

Fig. 4. Summary of the role of *chinmo* in insect metamorphosis. (*A*) Summary of the temporal progression of expression of Chinmo, Broad, and E93 in larval and imaginal cells of wild type and *chinmo* null mutants. (*B*) Relationship of the network for the three master genes that comprise the "trinity" that regulates the three major stages in the life history of *Drosophila.* Mutual inhibition can lock the insect in each of the three stages, but epigenetic information supplied by hormones and growth factors can shift the animal from one stable state to another. (*C*) Hypothesis for the relationship of the members of the trinity to life history of insects that show a direct development pattern that would be expected in the ancestor of the Holometabola. See text for details.

body. *Chinmo* expression then continues at high levels until "critical weight," the growth-related checkpoint that allows the preparation for metamorphosis (30, 36). After this checkpoint, larval tissues, such as the fat body (37) and the salivary glands (38), shift to making proteins necessary for metamorphosis, and imaginal discs switch from simple nutrient-dependent growth to the morphogenetic programs that results in disc patterning (36). For both larval cells (Fig. 1*E*) and imaginal discs (Fig. 1*D*) (28), the down-regulation of *chinmo* after the critical weight checkpoint is accompanied by the up-regulation of *broad*. In the discs, it has been shown that this change from Chinmo to Broad is essential for the discs to shift from self-renewal growth that allows disc regeneration in response to injury to differentiative growth that can support only simple wound healing (28).

The late embryonic blockage seen when the *chinmo* locus is completely removed through overlapping deletions shows that a larva can form in the absence of zygotically derived *chinmo* transcripts. However, Chinmo appears necessary to maintain larval function: salivary gland cells lacking Chinmo show retarded growth (Fig. 3*F*) and Chinmo-negative epidermal cells respond to the L1 ecdysteroid surge by trying to make a puparium rather than by making a second instar cuticle (Fig. 3 *D* and *E*). In young imaginal discs, the lack of Chinmo causes their cells to form a thickened epithelium that resembles that seen as a prelude to metamorphosis (Fig. 3*H*). We do not yet know whether these effects of the lack of Chinmo are direct responses to the loss of this factor or are indirect responses caused by the precocious appearance of E93 and Broad in larval and imaginal cells, respectively.

The striking feature of the removal of Chinmo is the precocious expression of the two key metamorphic genes, *broad* and *E93* (summarized in Fig. 4*A*). A switch from Chinmo and Broad expression at critical weight has been known for a while for both young neurons (27) and imaginal discs (28). These two genes reciprocally inhibit each other's expression around this time (28) and this transcriptional shift is reinforced by the *Let-7* family of microRNAs that stabilize *broad* transcripts and destabilize those of *chinmo* (39). We find, though, that a requirement for Chinmo to suppress *broad* expression extends back to the L1 stage when the imaginal discs begin their proliferation. The function of Chinmo in suppressing *E93* expression occurs even earlier, being evident from midembryogenesis (Fig. 2*F*), around when Chinmo first appears. We do not know if this is also a reciprocal relationship in which E93 can suppress expression of *chinmo*.

The gene network that supports the progression from larva to pupa to adult is depicted in Fig. 4*B*. As proposed by Williams and Kafatos (12), each of the master genes strongly influences the expression of the others. The known interactions are all inhibitory, as detailed above, although there is not yet experimental evidence to support the inhibition of *E93* by Broad or of *chinmo* by E93. Once established, each node of the network is inherently stable due to these inhibitory interactions but extrinsic factors, largely supplied by hormones, such as the ecdysteroids and juvenile hormone, and morphogens, like myoglianin (40, 41), can shift the animal from one node to the next, thereby allowing a metamorphic transition.

What, then, is the role of the trinity in insects that show direct development (Fig. 4*C*)? The function of E93 is the same in insects that show direct development and those that have complete metamorphosis. E93 is required at the end of somatic growth to transition into a reproductive stage (19–21). The

somatic growth of direct developing insects occurs through the nymphal stages which display the species-typical body plan throughout. In insects with complete metamorphosis, though, somatic growth occurs in a modified larval form, and the species-typical body plan organizes at the end of growth with formation of the pupa. In both cases, Broad is associated with the appearance of the species-typical body plan. In the latter case of complete metamorphosis, Broad appears toward the end of growth and is essential for generating the pupa. In direct developing insects, by contrast, *broad* appears early in embryogenesis (17, 18), and suppression of embryonic *broad* by maternal RNAi in the milkweed bug, *Oncopeltus fasciatus*, and the cockroach, *Blattella germanica*, results in a substantial percentage of embryos that do not progress beyond the extended germband stage (17, 18). This blockage point is important because it is where direct development and metamorphic development diverge with the former progressing to its species-typical form and the latter diverted to making a larval form. Chinmo then functions in *Drosophila* to maintain this larval form and to inhibit expression of both *broad* and *E93* until the end of the growth period. The developmental consequences of the relationship of *chinmo* with *broad* are elegantly shown by their functions in *Drosophila* imaginal discs where they provide the molecular gate that allows the discs to shift from simple growth to patterning and cell determination at critical weight (28). The only data on *chinmo* in direct developing insects are transcriptomic data in embryos of *B. germanica* (42): *chinmo* transcripts are prominent very early in embryogenesis but then decline between embryonic day 1 and 2 as the embryonic germ-band forms and *broad* transcripts increase. This timing and temporal relationship with Broad is consistent with a scenario in which Chinmo supports early embryonic growth and antagonizes the shift to embryonic patterning and cell determination. It will be crucial to understand how *chinmo* and *broad* interact in insects with direct development and what may have changed in this interaction to allow the maintenance of Chinmo and direct embryonic development away from making the species-typical form to making a larva instead.

Materials and Methods

Fly Strains and Rearing. *SI Appendix*, Table S1 shows the fly strains used, the abbreviations used in the text to designate the strains and the Bloomington Stock Center numbers. The Canton S strain used originated from the Canton S stock at the Department of Genetics, University of Cambridge in 1987 and has been maintained since then in the authors' laboratories.

Flies were maintained in 12:12 light:dark (L:D) photoperiod at 25 °C on standard *Drosophila* medium. The crosses of *UAS-RNAi* lines to the *en-GAL4*, *UAS-nRFP/CyO* line were reared at 29 °C, 12L:12D to enhance the effectiveness of the RNAi-mediated knockdown.

Immunocytochemistry and Imaging. Tissues were dissected and fixed in 3.9% formaldehyde (Thermo Fisher Scientific) in phosphate-buffered saline (PBS; Fisher Scientific) for 30–60 min, then rinsed and incubated in PBS-1% Triton X (TX; Fisher Scientific) with 2% normal donkey serum (Jackson ImmunoResearch) for 15–30 min. They were then incubated in PBS-1% TX with primary antibodies for 2–3 d at 4 °C, repeatedly rinsed, then incubated with secondary antibodies over one to two nights at 4 °C. Primary antibodies used were: rat anti-Chinmo polyclonal (43) at 1:1,000 dilution (gift of N. Sokol, University of Indiana); mouse anti-Broad core monoclonal (44) at 1:50 dilution (Mab 25E9.D7; Developmental Systems Hybridoma Bank, Iowa City); guinea pig anti-E93 (22) at 1:1,000 dilution (gift of C. Doe, University of Oregon). Other tissue stains were propidium iodide (Thermo Fisher Scientific, 1:1,000 dilution of 1 mg/mL stock) for DNA; Alexa-488 conjugated phalloidin (Thermo Fisher Scientific, 1:100 dilution of 200 units/mL stock in methanol) for actin; and Calcofluor White (Sigma Chemical) for cuticle.

Secondary antibodies were various Alexa Fluor 488-, 594-, or 647-conjugated donkey antisera raised against rabbit, mouse, rat, or guinea pig IgG fractions and used at 1:500 (Jackson ImmunoResearch Laboratories, West Grove, PA). Immunostained preparations were mounted on poly-L-lysine (Sigma-Aldrich) coated coverslips, dehydrated through a graded ethanol series, cleared in xylene and mounted in DPX (Sigma-Aldrich). The preparations were imaged on a Zeiss 800 confocal microscope and processed with ImageJ software (https://imagej.nih.gov/ij/).

Data Availability. All study data are included in the article and/or Supporting Information. Immunocytochemical image data is available from the authors on request.

ACKNOWLEDGMENTS. We thank Dr. Chris Q. Doe, University of Oregon, and Dr. Nicholas Sokol, Indiana University, for generously providing antibody reagents. Other antibodies were obtained from the Developmental Systems Hybridoma Bank (Iowa City) and the *Drosophila* stocks from the Bloomington Drosophila Stock Center. We thank Drs. Richard Strathmann, Victoria Foe, Jason Hodin, Rachel Merz, Brian Clark, and Barbora Konopova for critical comments on the manuscript. Funding was a gift from the Howard Hughes Medical Institute to the University of Washington to support the research of J.W.T.

1. X. Belles, *Insect Metamorphosis. From Natural History to Regulation of Development and Evolution* (Elsevier/Academic Press, London, 2020).
2. J. L. Rainford, M. Hofreiter, D. B. Nicholson, P. J. Mayhew, Phylogenetic distribution of extant richness suggests metamorphosis is a key innovation driving diversification in insects. *PLoS One* **9**, e109085 (2014).
3. J. W. Truman, The evolution of insect metamorphosis. *Curr. Biol.* **29**, R1252–R1268 (2019).
4. F. Sehnal, P. Švácha, J. Zrzavý, "Evolution of insect metamorphosis" in *Metamorphosis Postembryonic Reprogramming of Gene Expression in Amphibian and Insect Cells*, L. I. Gilbert, J. R. Tata, B. G. Atkinson, Eds. (Academic Press, 1996), chap. 1.
5. M. Jindra, Where did the pupa come from? The timing of juvenile hormone signalling supports homology between stages of hemimetabolous and holometabolous insects. *Philos. Trans. R. Soc. Lond. B Biol. Sci.* **374**, 20190064 (2019).
6. M. Jindra, X. Bellés, T. Shinoda, Molecular basis of juvenile hormone signaling. *Curr. Opin. Insect Sci.* **11**, 39–46 (2015).
7. B. Konopova, V. Smykal, M. Jindra, Common and distinct roles of juvenile hormone signaling genes in metamorphosis of holometabolous and hemimetabolous insects. *PLoS One* **6**, e28728 (2011).
8. A. Berlese, Intorno alle metamorfosi degli insetti. *Redia (Firenze)* **9**, 121–136 (1913).
9. J. W. Truman, L. M. Riddiford, The evolution of insect metamorphosis: A developmental and endocrine view. *Philos. Trans. R. Soc. Lond. B Biol. Sci.* **374**, 20190070 (2019).
10. A. S. Yang, Modularity, evolvability, and adaptive radiations: A comparison of the hemi- and holometabolous insects. *Evol. Dev.* **3**, 59–72 (2001).
11. I. M. Vea, C. Minakuchi, Atypical insects: Molecular mechanisms of unusual life history strategies. *Curr. Opin. Insect Sci.* **43**, 46–53 (2021).
12. C. M. Williams, F. C. Kafatos, Theoretical aspects of the action of juvenile hormone. *Mitt. Schweiz. Entomol. Ges.* **44**, 151–162 (1971). [Reprinted in *Insect Juvenile Hormones. Chemistry and Action.* J. J. Menn and M. Beroza, Eds. (Academic Press, 1972), 29-42.]
13. J. H. Willis, The paradigm of stage-specific gene sets in insect metamorphosis: Time for revision! Arch. Insect Biochem. Physiol. *Suppl.* **1**, 47–57 (1986).
14. F. D. Karim, G. M. Guild, C. S. Thummel, The *Drosophila Broad-Complex* plays a key role in controlling ecdysone-regulated gene expression at the onset of metamorphosis. *Development* **118**, 977–988 (1993).
15. X. Zhou, L. M. Riddiford, Broad specifies pupal development and mediates the 'status quo' action of juvenile hormone on the pupal-adult transformation in *Drosophila* and *Manduca*. *Development* **129**, 2259–2269 (2002).
16. D. F. Erezyilmaz, L. M. Riddiford, J. W. Truman, The pupal specifier *broad* directs progressive morphogenesis in a direct-developing insect. *Proc. Natl. Acad. Sci. U.S.A.* **103**, 6925–6930 (2006).
17. D. F. Erezyilmaz, M. R. Rynerson, J. W. Truman, L. M. Riddiford, The role of the pupal determinant *broad* during embryonic development of a direct-developing insect. *Dev. Genes Evol.* **219**, 535–544 (2009).
18. M.-D. Piulachs, V. Pagone, X. Bellés, Key roles of the *Broad-Complex* gene in insect embryogenesis. *Insect Biochem. Mol. Biol.* **40**, 468–475 (2010).
19. D. Martín, S. Chafino, X. Franch-Marro, How stage identity is established in insects: The role of the Metamorphic Gene Network. *Curr. Opin. Insect Sci.* **43**, 29–38 (2021).
20. E. Ureña, C. Manjón, X. Franch-Marro, D. Martin, E93 specifies adult metamorphosis in insects. *Proc. Natl. Acad. Sci. U.S.A.* **111**, 7024–7029 (2014).
21. S. Chafino *et al.*, Upregulation of E93 gene expression acts as the trigger for metamorphosis independently of the threshold size in the beetle *Tribolium castaneum*. *Cell Rep.* **27**, 1039–1049.e2 (2019).
22. B. Zhou, D. W. Williams, J. Altman, L. M. Riddiford, J. W. Truman, Temporal patterns of *broad* isoform expression during the development of neuronal lineages in *Drosophila*. *Neural Dev.* **4**, 39 (2009).
23. F. Pecasse, Y. Beck, C. Ruiz, G. Richards, Krüppel-homolog, a stage-specific modulator of the prepupal ecdysone response, is essential for *Drosophila* metamorphosis. *Dev. Biol.* **221**, 53–67 (2000).

24. T. Daimon, M. Uchibori, H. Nakao, H. Sezutsu, T. Shinoda, Knockout silkworms reveal a dispensable role for juvenile hormones in holometabolous life cycle. *Proc. Natl. Acad. Sci. U.S.A.* **112**, E4226–E4235 (2015).
25. M. H. Syed, B. Mark, C. Q. Doe, Steroid hormone induction of temporal gene expression in *Drosophila* brain neuroblasts generates neuronal and glial diversity. *eLife* **6**, e26287 (2017).
26. S. Zhu *et al.*, Gradients of the *Drosophila* Chinmo BTB-zinc finger protein govern neuronal temporal identity. *Cell* **127**, 409–422 (2006).
27. C. Maurange, L. Cheng, A. P. Gould, Temporal transcription factors and their targets schedule the end of neural proliferation in *Drosophila*. *Cell* **133**, 891–902 (2008).
28. K. Narbonne-Reveau, C. Maurange, Developmental regulation of regenerative potential in *Drosophila* by ecdysone through a bistable loop of ZBTB transcription factors. *PLoS Biol.* **17**, e3000149 (2019).
29. S. E. Celniker *et al.*; modENCODE Consortium, Unlocking the secrets of the genome. *Nature* **459**, 927–930 (2009).
30. C. Mirth, J. W. Truman, L. M. Riddiford, The role of the prothoracic gland in determining critical weight for metamorphosis in *Drosophila melanogaster*. *Curr. Biol.* **15**, 1796–1807 (2005).
31. S. Cohen, "Imaginal disc development" in *The Development of Drosophila melanogaster*, M. Bate, A. Martinez Arias, Eds. (Cold Spring Harbor Laboratory Press, Plainview, 1993), vol. **2**, chap. 13.
32. C. M. Uyehara *et al.*, Hormone-dependent control of developmental timing through regulation of chromatin accessibility. *Genes Dev.* **31**, 862–875 (2017).
33. M. J. Niederhuber, D. J. McKay, Mechanisms underlying the control of dynamic regulatory element activity and chromatin accessibility during metamorphosis. *Curr. Opin. Insect Sci.* **43**, 21–28 (2021).
34. S. L. Nystrom, M. J. Niederhuber, D. J. McKay, Expression of E93 provides an instructive cue to control dynamic enhancer activity and chromatin accessibility during development. *Development* **147**, dev181909 (2020).
35. K. Sander, Specification of the basic body pattern in insect embryogenesis. *Adv. Insect Physiol.* **12**, 125–238 (1976).
36. C. K. Mirth, J. W. Truman, L. M. Riddiford, The ecdysone receptor controls the post-critical weight switch to nutrition-independent differentiation in *Drosophila* wing imaginal discs. *Development* **136**, 2345–2353 (2009).
37. J.-A. Lepesant *et al.*, Developmentally regulated gene expression in *Drosophila* larval fat bodies. *J. Mol. Appl. Genet.* **1**, 371–383 (1982).
38. E. M. Meyerowitz, K. Vijay Raghavan, P. H. Mathers, M. Roark, How *Drosophila* larvae make glue: Control of Sgs-3 gene expression. *Trends Genet.* **3**, 288–293 (1987).
39. Y. C. Wu, G. Chawla, N. Sokol, *let-7-Complex* microRNAs regulate Broad-Z3, which together with Chinmo maintains adult lineage neurons in an immature state. *G3 (Bethesda)* **10**, 1393–1401 (2020).
40. O. Kamsoi, X. Bellés, Myoglianin triggers the premetamorphosis stage in hemimetabolan insects. *FASEB J.* **33**, 3659–3669 (2019).
41. L. L. He *et al.*, Mechanism of threshold size assessment: Metamorphosis is triggered by the TGF-beta/Activin ligand Myoglianin. *Insect Biochem. Mol. Biol.* **126**, 103452 (2020).
42. G. Ylla, M.-D. Piulachs, X. Bellés, Comparative transcriptomics in two extreme neopterans reveals general trends in the evolution of modern insects. *iScience* **4**, 164–179 (2018).
43. G. Chawla, P. Deosthale, S. Childress, Y. C. Wu, N. S. Sokol, A *let-7-to-miR-125* microRNA switch regulates neuronal integrity and lifespan in *Drosophila*. *PLoS Genet.* **12**, e1006247 (2016).
44. I. F. Emery, V. Bedian, G. M. Guild, Differential expression of *Broad-Complex* transcription factors may forecast tissue-specific developmental fates during *Drosophila* metamorphosis. *Development* **120**, 3275–3287 (1994).